Prediction of charge separation in GaAs/AlAs cylindrical nanostructures

Jeongnim Kim, Lin-Wang Wang, and Alex Zunger

National Renewable Energy Laboratory, Golden, Colorado 80401

(Received 13 August 1997)

It is known that in a sequence of flat, type-I $(GaAs)_m/(AlAs)_n/(GaAs)_p/(AlAs)_q \cdots$ multiple quantum wells (MQWs), the wave functions of both the valence-band maximum and the conduction-band minimum are localized on the widest well. Thus, electron-hole charge separation is not possible. On the other hand, for short-period superlattices (type II), the electron and hole are localized on different materials (electron on AlAs and hole on GaAs) and different band-structure valleys (hole at Γ and electron at X). Using a plane-wave pseudopotential direct-diagonalization approach, we predict that electron-hole charge separation on different layers of the *same* material (GaAs) and *same* valley (Γ) is possible in *curved* (but not in flat) *geometries*. This is predicted for a set of concentric, nested cylinders of GaAs and AlAs (Russian Doll). Since the flat multiple-quantum-well structure and the Russian Doll structure with the same layer thicknesses have the same band offset diagram, the difference in behavior is not due to the potential. Rather, it reflects different interband coupling and kinetic energy confinement induced by the *curvature*, present in the nested-cylinder geometry but absent in the MQW. This identifies a geometric degree of freedom (curvature) that can be used to tailor electronic properties of nanostructures. [S0163-1829(97)51644-4]

Recent advances in nanotechnology permit fabrication of complex nanostructures with special electronic and optical properties reflecting dimensional confinement on a nanometer scale,[1,2] e.g., multiple quantum wells[3] and core-shell structures.[4] The essential building blocks of such structures are alternating layers of different semiconducting materials, acting as ''wells'' and ''barriers,'' and controlling the confinement energies and thus the localization of charge carriers. The materials comprising the wells and barriers are usually flat, two-dimensional semiconductor films,[3] stacked like a deck of cards to produce ''multiple quantum wells (MQWs)'' or ''superlattices.'' In this case, wave functions of the conduction-band minimum (CBM) and valence-band maximum (VBM) at the Brillouin zone center, are localized on the *widest wells*, having the lowest confinement energy.[3,5] Consequently, it is normally impossible to create a sequence of flat layers that would exhibit separation of charge carriers on different layers of the *same material*. When electron-hole charge separation does exist, it is found that the electron and the hole are localized on *different materials*, as in ''type-II'' superlattices[6] (e.g., electrons in AlAs and holes in GaAs). Similarly, ''charge transfer'' transitions in inorganic solids[7] involve localization of electrons and holes on different atoms or chemical groups within the solid (e.g., on the ligand and on the core metal, respectively). Since nonplanar geometry of multiple-quantum wells, envisioned by Watanabe[8] and discussed by Tatarinova *et al.*[9], are now realized via ''core-shell structures,''[4] we were wondering if utilization of such distinct geometric degrees of freedom could affect charge separation of electrons and holes on different layers of the *same* material (e.g., GaAs).

We have thus contrasted the quantum confinement of (i) multiple quantum wells of *flat* GaAs and AlAs layers, i.e., $(GaAs)_m/(AlAs)_n/(GaAs)_p/(AlAs)_q$, with (ii) nested cylinders—an equivalent sequence of wells and barriers arranged as *concentric wires* (Russian Doll) (Fig. 1). Using a pseudopotential plane-wave calculation, we identified a set of periods ($m,n,p,$ and q) such that charge separation can exist in nested cylindrical structures: the CBM is localized in

the inner (mth) GaAs layer, while the VBM is localized in the outer (pth) GaAs layer. In contrast, the band edge states of linear multiple quantum wells with equivalent layer thickness do not exhibit any charge separation. Thus, a Russian Doll geometry provides a charge separation that is impossible with equivalent linear multiple quantum wells. This
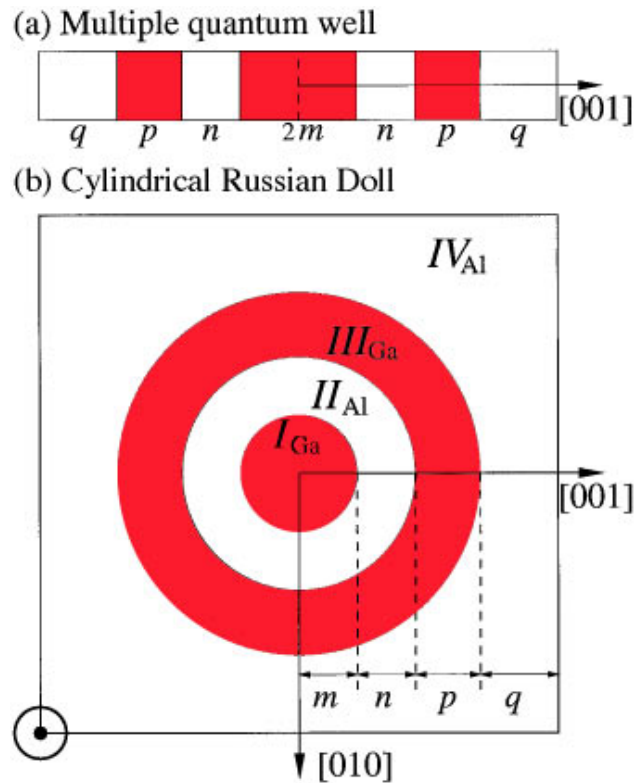

FIG. 1. (Color). Schematics of structure of (a) (001) multiple quantum wells, and (b) a {100} cross-section of an equivalent nested cylinder. These structures are made of alternating GaAs (red) and AlAs segments with thicknesses m, n, p, and q monolayers, respectively, in the order (starting from the center) $I_{Ga} \rightarrow II_{Al} \rightarrow III_{Ga} \rightarrow IV_{Al}$.
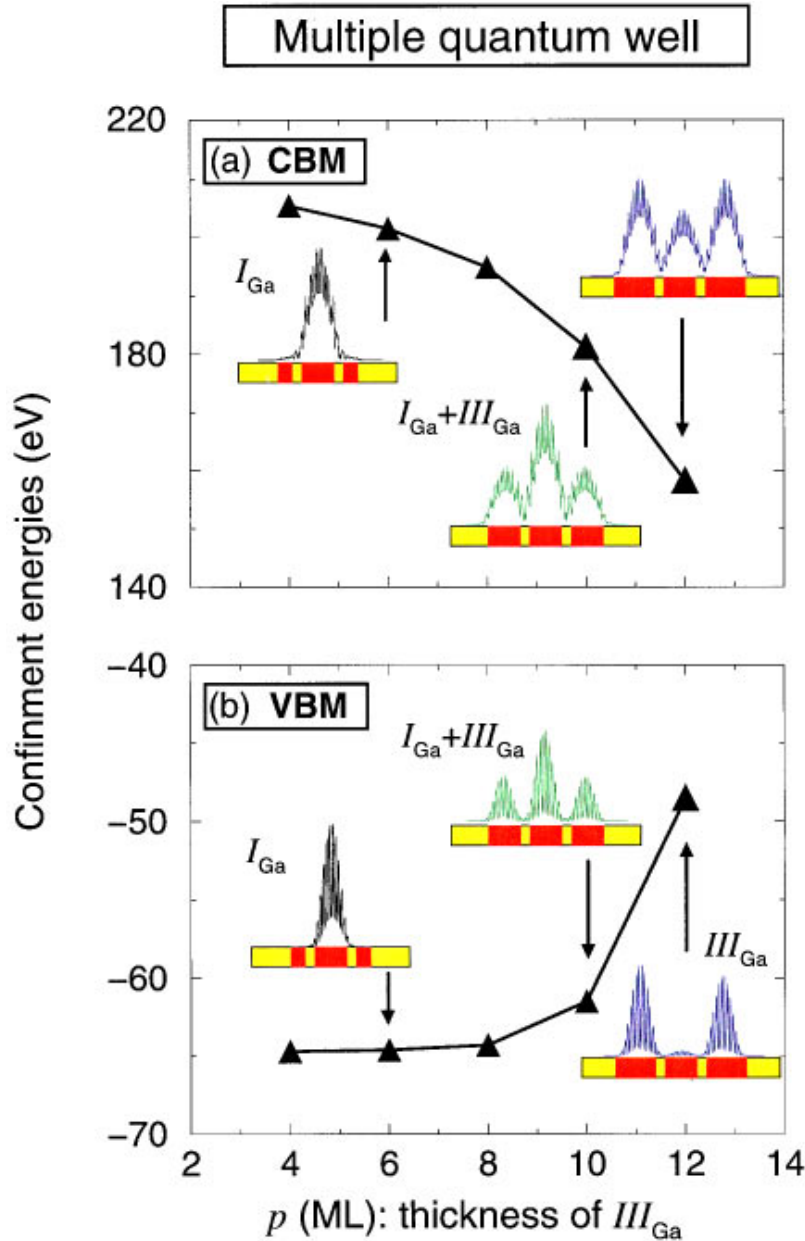
FIG. 2. (Color). Confinement energies (triangles) and wave-function amplitudes (insets) of the (a) CBM and (b) VBM of linear multiple quantum wells, as a function of the thickness $p(III_{Ga})$ of the outer GaAs layer. Other thicknesses are fixed at $m(I_{Ga}) = 5$ ML, $n(II_{Al}) = 4$ ML and $q(IV_{Al}) = 8$ ML. Red (yellow) denotes a GaAs (AlAs) layer.

study thus identifies a new geometric degree of freedom (curvature) that can be used to manipulate electronic properties of nanostructures.[10]

The electronic structure of the nanostructures is described here using a direct-diagonalization (multiband) approach to the single-particle Schrödinger equation,

$$\left\{ -\tfrac{1}{2} \nabla^2 + \sum_{n\alpha} v_\alpha(|\mathbf{r} - \mathbf{d}_\alpha - \mathbf{R}_n|) \right\} \psi_i(\mathbf{r}) = \epsilon_i \psi_i(\mathbf{r}), \quad (1)$$

where v_α is the screened pseudopotential of atom of type α located at site $\mathbf{d}_\alpha$ within cell $\mathbf{R}_n$. The pseudopotential is fit to the measured bulk band structures and to the *ab initio* bulk wave functions.[11] The potential used here accurately describes type-I/type-II transitions in ordered AlAs/GaAs superlattices[6] as well as the bowing in bulk $Al_x Ga_{1-x}As$

random alloys[11] and wave function localization in disordered superlattices.[12] We use the ''folded spectrum method''[13] to find the band edge eigenstates of Eq. (1). Its linear scaling with the number of atoms allows us to handle easily systems of $10^3 - 10^4$ atoms.

Figure 2 shows the calculated confinement energies of the conduction-band minimum and the valence-band maximum of *linear multiple quantum wells* as a function of the thickness $p(III_{Ga})$ of the outer GaAs segment (see Fig. 1 for a definition of the structure). Confinement energies are defined with respect to CBM and VBM of bulk GaAs. The thickness of the innermost GaAs segment is fixed at $m(I_{Ga}) = 5$ monolayers (ML). Figure 2 also shows the wave function amplitudes of the nanostructures, so that the localization can be assessed. The red bars denote AlAs layers, while the yellow
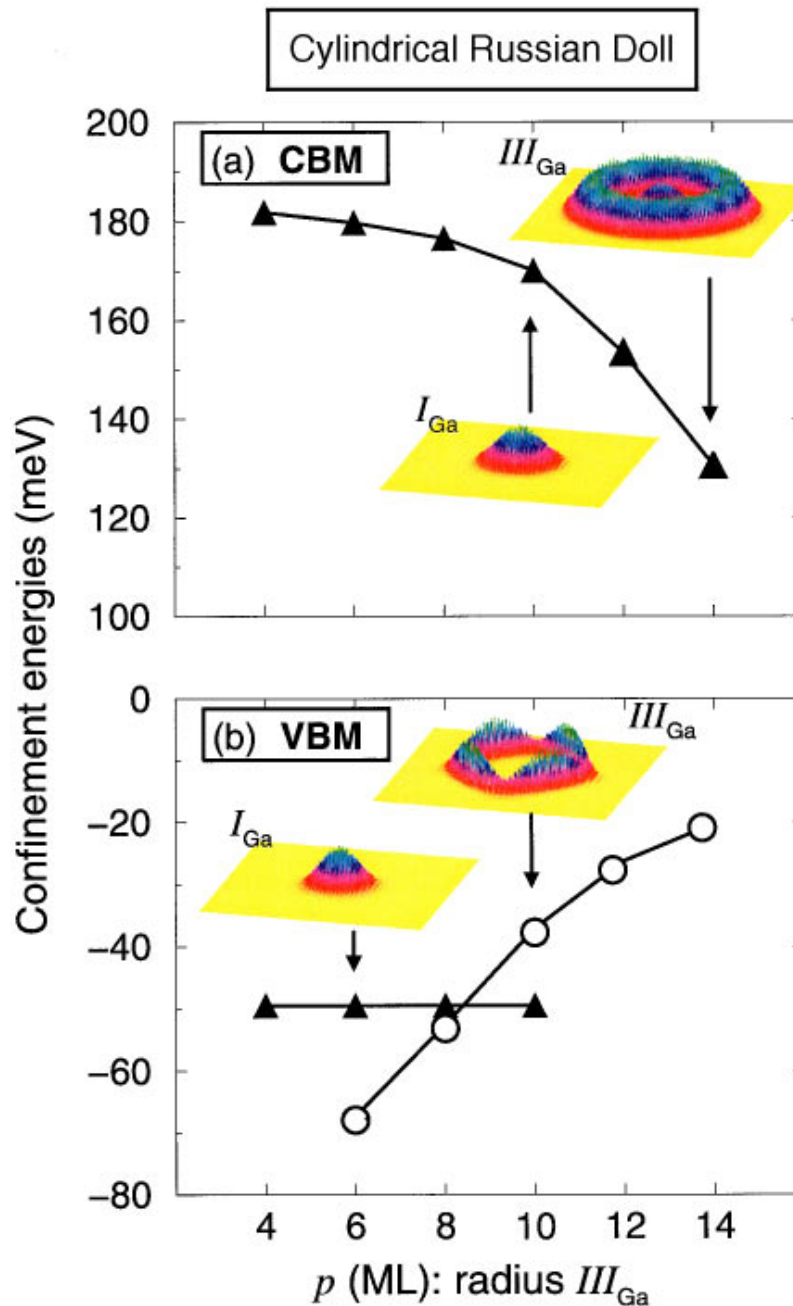
FIG. 3. (Color). Confinement energies of the (a) CBM and (b) two highest valence bands for nested cylinders vs the thickness $p(III_{Ga})$. The other parameters are held fixed at $m = 10$ ML, $n = 4$ ML and $q = 8$ ML. Wave-function amplitudes, averaged along the wire direction, are shown as insets for a few structures.

bars denote GaAs layers. We see that, as expected, both the CBM and VBM are localized on the widest wells. Wave functions are localized on the innermost GaAs segment (I_{Ga}) when layer III_{Ga} is below 10 ML. They are localized on the III_{Ga} segment when layer III is thicker than the innermost layer, i.e., $p > 2m$. When the two GaAs wells, I_{Ga} and III_{Ga}, have the same thickness, $p = 2m$, the CBM and VBM have equal amplitudes in the two wells. Since the wells I_{Ga} and III_{Ga} have the same potential depths determined by bulk band offsets, the transition from localization in I_{Ga} to localization in III_{Ga} is purely due to the confinement: it occurs when the kinetic confinement energy in well III_{Ga} becomes smaller to that in well I_{Ga}.

Figure 3 shows the confinement energies of the CBM and VBM in the Russian Dolls as a function of $p(III_{Ga})$; the thicknesses of other layers are fixed as before. Similar to the MQW case of Fig. 2, both the CBM and VBM are localized in I_{Ga} when $p(III_{Ga}) < zm(I_{Ga})$ and in III_{Ga} when $p(III_{Ga}) > zm(I_{Ga})$. However, in contradiction to the MQW case, we observe a charge separation for $p(III_{Ga}) = zm(I_{Ga}) = 10$ ML: the CBM is localized in I_{Ga}, while the VBM is localized in III_{Ga}. We find the same charge separation when $p(III_{Ga}) = m(I_{Ga}) = 12$ ML. Thus a curved geometry of nested wells affords electron-hole separation on different layers of the same material.

Charge separation occurs when the confinement energies

of the two valence states [triangles and circles in Fig. 4(b)] cross. The two valence states of the nested cylinders in Fig. 3(b) have different nodal structures and angular momenta: In cylindrical coordinates $\rho, \phi, z = [001]$, we can express the valence wave functions in terms of bulk wave functions at Brillouin zone center (u_i where $i = x$, y, and z) and envelope functions $e^{\pm i m_z \phi} f_{m_z}(\rho)$. Under spherical approximation of the bulk Hamiltonian, the wave functions marked in Fig. 3(b) by triangles can be written as $u_z f_0(\rho)$, where $m_z = 0$. Thus, $f_0(\rho)$ has its *maximum* at the center $\rho = 0$. On the other hand, the wave functions marked in Fig. 3(b) by circles can be expressed as $[(u_x + iu_y)e^{-i\phi} + (u_x - iu_y)e^{i\phi}]f_1(\rho)$. The angular momentum of this state constrains the amplitude of $f_1(\rho)$ to be *zero* at $\rho = 0$ and introduces a centrifugal potential proportional to m_z^2/ρ^2 with $m_z = 1$. Therefore, the valence states with $m_z = 1$ favors localization far from the center, while the state with $m_z = 0$ lacks any centrifugal potential, so it localizes at the center. Note that, both the states marked in Fig. 3(b) by triangle and circle have a zero z component of the total angular momentum. Thus, they are both singlet states. Charge separation occurs when the thickness $p(III_{Ga})$ is large enough so that the kinetic confinement of the valence states of $m_z = 1$ is more favorable in layer III_{Ga} than that of states of $m_z = 0$ in layer I_{Ga}. In contrast to this behavior, in MQWs, the potential depths are the same in two GaAs wells, regardless of the spatial symmetry of the wave functions. The relative confinement energies in layer I_{Ga} and layer III_{Ga} are determined only by the well widths. Localization on the wider well is always favorable, and thus charge separation in different wells cannot be realized in linear MQW.

To compare quantitatively the different energy levels of the two structures, Table I gives the confinement energies of the CBM and VBM for a few structures of nested cylinders and linear multiple quantum wells at the same layer thicknesses. We see that given the same layer thicknesses, the confinement energies (ΔE) of Russian Doll cylinders are considerably larger than those of linear multiple quantum wells. This is due to the two-dimensional confinement nature of nested cylinders.

In all cases discussed so far, all band edge states are Γ derived. However, the bottom half of Table I shows that the CBM of Russian Dolls can be derived from the bulk X_{1c} state and is localized at region IV_{Al}. This is analogous to a

TABLE I. The confinement energies (ΔE in meV) of the CBM and VBM for various layer thicknesses, m, n, and P (in ML) of the cylindrical nested cylinders and multiple quantum wells. Band edge states are Γ-like, unless stated.

Layer thickness zm-n-p	State	Russian Dolls [a]		Quantum well [b]	
		ΔE	Localization	ΔE	Localization
10-4-4	CBM	181.9	I_{Ga}	84.8	I_{Ga}
	VBM	−49.4	I_{Ga}	−20.7	I_{Ga}
10-4-10	CBM	170.2	I_{Ga}	83.6	I_{Ga}
	VBM	−37.0	III_{Ga}	−20.7	I_{Ga}
6-4-4	CBM	216.1	IV_{Al} (X)	167.1	I_{Ga}
	VBM	−116.7	I_{Ga}	−48.7	I_{Ga}
6-4-6	CBM	215.8	IV_{Al} (X)	165.0	I_{Ga}
	VBM	−84.5	III_{Ga}	−48.7	I_{Ga}

[a]$q(IV_{Al}) = 10$ ML.
[b]$q(IV_{Al}) = 14$ ML.

type-I/type-II transition in superlattices.[6] It is well known that, when the thickness of a well is smaller than a critical thickness, the CBM is derived from the bulk X_{1c} state instead of the Γ_{1c} state.[5] This transition is found to occur at a different critical size depending upon the confinement dimension. Table I also shows a different $\Gamma - X$ crossing in MQW and nested cylinders. However, the critical size of the $\Gamma - X$ crossing is the same for the single-well and nested-well structures: the crossover diameter is about 20 ML for both the quantum wires and Russian Dolls, while the crossover thickness is about 10 ML for quantum wells and MQW.

In summary, we have shown that in analogy with nested (cylinder) carbon nanotubes,[14] where new physical properties, absent in the corresponding flat (graphite) sheets are attainable, ordinary semiconductor Russian Doll cylinder structures can also exhibit distinct properties, absent in flat multiple quantum wells. In particular, nested cylinder GaAs/AlAs structures afford charge separation on different sheets of the same material. Experimental testing of these new degrees of freedom are called for.

[1]*Nanostructures and Quantum Effects*, edited by H. Sakaki and H. Noge (Springer-Verlag, Heidelberg, 1993).

[2]*Optical Properties of Semiconductor Quantum Dots*, edited by U. Woggon (Springer-Verlag, Heidelberg, 1997).

[3]*Superlattices and Other Heterostructures: Symmetry and Optical Phenomena*, edited by E. L. Ivchenko and G. E. Pikus (Springer-Verlag, Berlin, Heidelberg, 1995).

[4]G. W. Bryant et al., Surf. Sci. **361/362** 801 (1996); M. A. Hines and P. Guyot-Sionnest, J. Phys. Chem. **100**, 468 (1996); H. S. Zhou et al., ibid. **97**, 895 (1993); D. Schooss et al., Phys. Rev. B **49**, 17 072 (1994); A. Mews et al., ibid. **53**, R13 242 (1996).

[5]A. Franceschetti and A. Zunger, Phys. Rev. B **52**, 14664 (1995).

[6]A. Ishibashi et al. J. Appl. Phys. **58**, 2691 (1985); G. Li et al., Phys. Rev. B **40**, 10 430 (1989).

[7]D. F. Shirver et al., *Inorganic Chemistries* (W. H. Freeman, New York, 1994), Vol. 590, p. 210.

[8]H. Watanabe, in *The Physics and Fabrication of Microstructures and Microdevices*, edited by M. J. Kelly and C. Weisbuch (Springer-Verlag, Heidelberg, 1986), p. 158.

[9]T. V. Tatarinova et al., Phys. Rev. B **50**, 17 349 (1994).

[10]D. M. Wood and A. Zunger, Phys. Rev. B **53**, 7949 (1996).

[11]K. A. Mäder and A. Zunger, Phys. Rev. B **50**, 17393 (1994).

[12]K. A. Mäder et al., Phys. Rev. Lett. **74**, 2555 (1995).

[13]L.-W. Wang and A. Zunger, J. Chem. Phys. **100**, 2394 (1994).

[14]*Science of Fullerenes and Carbon Nanotubes*, edited by M. Dresselhaus, G. Dresselhaus, and P. C. Eklund (Academic Press, San Diego, 1996).